Computers and Concrete, *Vol. 19, No. 6 (2017) 625-630*
DOI: https://doi.org/10.12989/cac.2017.19.6.625

Bond behavior between high volume fly ash concrete and steel rebars

Jiong-Feng Liang*[1,2], Ming-Hua Hu[2], Lian-Sheng Gu[2] and Kai-Xi Xue[2]

[1]*Jiangxi Engineering Research Center of Process and Equipment for New Energy, East China University of Technology, 418 Guanglan Road, Nanchang, P.R. China*
[2]*Faculty of Civil & Architecture Engineering, East China University of Technology, 418 Guanglan Road, Nanchang, P.R. China*

(Received August 22, 2016, Revised March 7, 2017, Accepted March 9, 2017)

Abstract. In this paper, 54 pull-out specimens and 36 cubic specimens with different replacement ratios of fly ash in the concrete (i.e., 0%, 20%, 30%, 40%, 50%, 60%) were fabricated to evaluate the bond at the interface between fly ash concrete and steel rebar. The results showed that the general shape of the bond-slip curve between fly ash concrete and steel rebar was similar to that for the normal concrete and steel rebar. The bond strength between fly ash concrete and the steel rebar was closer to each other at the same rebar diameter, irrespective of the fly ash replacement percentage. On the basis of a regression analysis of the experimental data, a revised bond strength mode and bond-slip relationship model were proposed to predict the bond-slip behaviour of high volume fly ash concrete and steel rebar.

Keywords: fly ash; concrete; bond-slip relationship; pull-out; strength

1. Introduction

In the past, cement production was a relatively significant source of global carbon dioxide (CO_2) emissions. And one of the solutions for this global concern was the use of supplementary cementitious materials as replacement of cement. The fly ash, a by-product of thermal power plants, has been considered as an ideal and available supplementary cementitious material.

The use of fly ash as alternative of Portland cement in concrete has been studied by many researchers. Junaid *et al.* (2015) studied the performance of fly ash based geopolymer concrete made by using non-pelletized fly ash aggregates after exposure to high temperatures. They found that most change to the strength and microstructure of geopolymer concrete occurred in the first few hours of exposure after which, the duration of heating had no significant effect. Shafigh *et al.* (2016) found that using high volume fly ash in oil palm shell concrete significantly reduced short-term mechanical properties, however, the use of limestone powder significantly improved the compressive strength at early and later ages. Shen *et al.* (2016) presented an experimental investigation on the tensile properties of hardening fly ash high strength concrete at different ages and quantified the uniaxial tensile strength and tensile Young's modulus of fly ash high strength concrete.

Leung *et al*. (2016) presented the surface water absorption of self-compacting concrete (SCC) containing fly ash and silica fume using sorptivity test. Assi *et al.* (2016) investigated the effects of activating solution type, curing procedure, and source of fly ash in relation to the resulting compressive strength of fly ash-based geopolymer concrete.

Chousidis *et al.* (2015) presented the effect of Greek fly ash as a partial replacement of cement, on the durability and mechanical resistance of reinforced concrete immersed in sodium chloride (NaCl) solution. Wang and Park (2015) presented a numerical procedure to evaluate the compressive strength development of high-volume fly ash concrete. Nath and Sarker (2015) studied fly ash based geopolymer concrete suitable for ambient curing condition. A small proportion of ordinary Portland cement (OPC) was added with low calcium fly ash to accelerate the curing of geopolymer concrete instead of using elevated heat. Tang (2015) studied the local bond stress-slip behavior of reinforcing bars embedded in lightweight aggregate concrete. The results showed that the ultimate bond strength increased with the increase of concrete compressive strength. Deng *et al.* (2014) investigated the bonding properties between high strength rebar and reactive powder concrete.

However, the bond-slip behavior between steel rebar and fly ash concrete is rarely reported. In this study, the purposes are to investigate bond-slip behavior for steel rebar in high-volume fly ash concrete.

2. Experimental programme

2.1 Materials and mix proportions

Ordinary Portland cement with a 28 day compressive strength of 42.5 MPa was used in this investigation. And another cementitious material was Class C fly ash according to ASTM, the chemical compositions of which were presented in Table 1.

The coarse aggregate is natural coarse aggregates, which in the range 5-20 mm. The fine aggregate is river sand with

*Corresponding author, Ph.D.
E-mail: jiongfeng108@126.com

ISSN: 1598-8198 (Print), 1598-818X (Online)

Table 1 Chemical compositions of fly ash

SiO_2	Al_2O_3	Fe_2O_3	CaO	MgO	$S0_3$	Others
49.1	31.5	6.9	4.9	0.8	1.2	5.6

Table 2 Mix proportion of the fly ash concrete

No.	Replacement (%)	Fly ash ($kg \cdot m^{-3}$)	Cement ($kg \cdot m^{-3}$)	Sand ($kg \cdot m^{-3}$)	Coarse aggregate ($kg \cdot m^{-3}$)	Water ($kg \cdot m^{-3}$)	Water admixtures ($kg \cdot m^{-3}$)
F0	0	0	430	533	1287	180	3.7
F20	20	86	344	533	1287	180	3.7
F30	30	129	301	533	1287	180	3.7
F40	40	172	258	533	1287	180	3.7
F50	50	215	215	533	1287	180	3.7
F60	60	258	172	533	1287	180	3.7

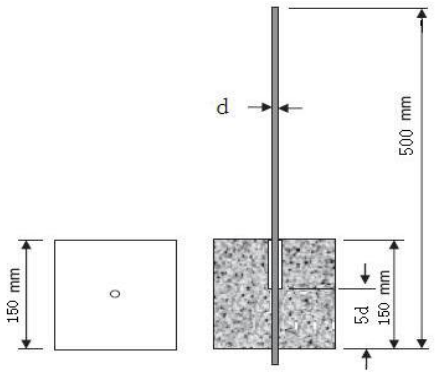

Fig. 1 Dimensions of test specimens

fineness modulus of 2.7. The deformed steel bar (HRB335) of 12 mm, 16 mm and 20 mm diameter were used in this pullout tests. Table 2 provides the design of the concrete mix, which were designed with varying the replacement ratio of fly ash (FA) in the concrete (i.e., FA replaced 0, 20, 30, 40, 50 and 60% of cement in the concrete, respectively.)

2.2 Specimens preparation and curing

The preparation and the cure of all the mixes are conducted in the State Key Laboratory for Concrete Material Research at East China Institute of Technology in Nanchang, PR China. Pull-out specimens are designed according to Chinese Standard Methods for Testing of Concrete Structures (GB 5015292) (1992). Each specimen consisted of a 150mm concrete cube with a single rebar is embedded vertically along a central axis. Steel rebars were embedded in the concrete cubes with a bonded length of five times the bar diameter as shown in Fig. 1. In order to control the bonded length, the steel rebars are prepared with a bond breaker using soft PVC tubes inserted around the bar to prevent contact of steel rebars with concrete. And the PVC tubes are placed at the loaded end side to minimize the effect of the stress from loading plate. In total, 54 pull-out specimens are prepared. And 36 cubic specimens are also prepared to determine the compressive strength and splitting tensile strength. All the specimens are demolded a day after pouring and transferred to the curing room under natural conditions for 28 days.

Fig. 2 Test setup

Table 3 Experiment results of the pullout specimens

Specimen	f_{cu} (MPa)	f_t (MPa)	P_{max} (kN)	τ_{max} (MPa)	Unloaded end slip (mm)
S12F0	49.9	2.77	58.1	25.7	1.27
S12F20	33.7	2.69	58.3	25.8	1.24
S12F30	31.6	2.59	57.4	25.4	1.26
S12F40	28.5	2.53	56.7	25.1	1.19
S12F50	26.7	2.46	58.6	25.9	1.18
S12F60	25.9	2.41	57.7	25.5	1.09
S16F0	49.9	2.77	68.7	17.1	0.72
S16F20	33.7	2.69	66.7	16.6	0.73
S16F30	31.6	2.59	69.9	17.4	0.77
S16F40	28.5	2.53	69.1	17.2	0.76
S16F50	26.7	2.46	67.9	16.9	0.73
S16F60	25.9	2.41	64.7	16.1	0.72
S20F0	49.9	2.77	83.5	13.3	0.64
S20F20	33.7	2.69	80.4	12.8	0.57
S20F30	31.6	2.59	77.9	12.4	0.53
S20F40	28.5	2.53	77.2	12.3	0.54
S20F50	26.7	2.46	74.1	11.8	0.56
S20F60	25.9	2.41	72.8	11.6	0.55

2.3 Testing

The loading setup for the pullout test is a UTM-300 microcomputer controlled electro-hydraulic servo tester, as shown in Fig. 2. The pullout is applied through a displacement control rate of 1 mm/min is chosen to comply with GB 5015292 maximum rate of 12 kN/min. The load is measured with the electro-hydraulic servo tester. The free-end slip of the steel rebar relative to concrete is measured using a LVDT(Linear Variable Differential Transformer).

3. Results and discussion

3.1 Mechanical properties of the HVFAC

The experiment results of the pullout specimens,

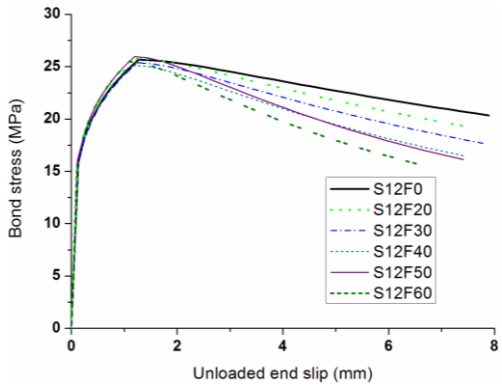

Fig. 3 Relationship between bond stress and slip for the 12 mm dia. bars

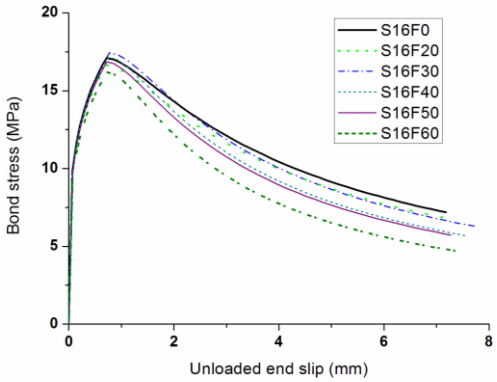

Fig. 4 Relationship between bond stress and slip for the 16 mm dia. bars

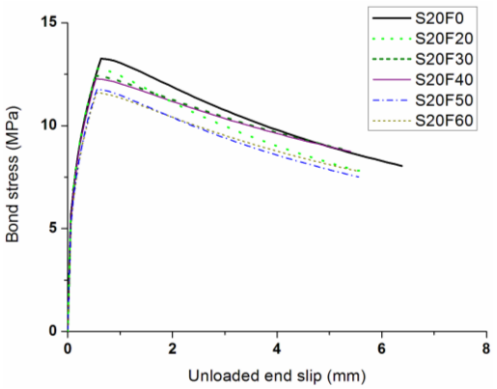

Fig. 5 Relationship between bond stress and slip for the 20 mm dia. bars

including compressive strength f_{cu}, splitting tensile strength f_t of high volume fly ash concrete(HVFAC), peak load P_{max}, peak bond stress τ_{max} and Unloaded end slip are summarized in Table 3. As shown in Table 3, the volume of fly ash has certain effect on compressive strength and splitting tensile strength of fly ash concrete. The compressive strength and splitting tensile strength of fly ash concrete declines with the increase of the volume of fly ash.

3.2 Relationship between bond stress and slip

The relationship between bond stress and slip for the 12 mm, 16 mm and 20 mm diameter rebars is presented in

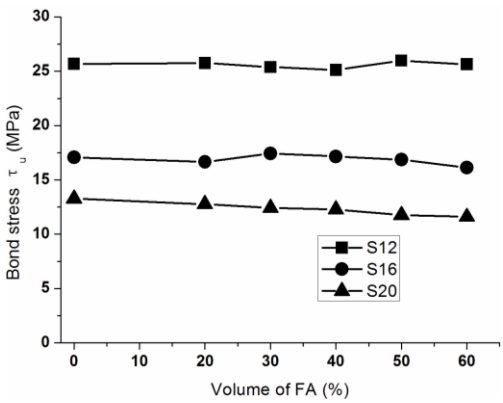

Fig. 6 Effect of the volume of fly ash on bond strength

Figs. 3-5, respectively. Each curve reflects the behavior at different stages which are micro-slip, internal cracking, descending. At the micro-slip stage, the load is small and no obvious slip occurs at the free end of the rebar, and the bond-slip curve which was sharply ascending remains linear. After that, at the internal cracking stage, the rebar begin to slip when the load increase towards a critical value, which indicates that the adhesion force at the anchorage has nearly been exhausted. This phase is characterized by an increase in the rate of slip in which the ascending branch of the bond-slip curve become distinctly nonlinear, and then the bond stress reaches the peak bond stress. At the descending stage, the bond stress declines rapidly and the slip increase with bond being attribute to the bearing and friction between the rebar and fly ash concrete. Figs. 3-5 indicate that no great differences in the bond-slip curves. This indicate the inclusion of fly ash do not modify the bond mechanisms and therefore the bond development and deterioration process between the high volume fly ash concrete and the steel rebar is similar to that between the natural concrete and steel rebar.

3.3 Bond strength

During the pullout test, the pullout load and steel rebar are recorded. The pullout load is then converted into bond stress according to the embedment length and steel rebar perimeter using Eq. (1)

$$\tau_u = \frac{P_u}{\pi d l_a} \tag{1}$$

where τ_u is the peak bond stress (MPa) between concrete and steel rebar which is also termed the bond strength; P_u is the peak load (N); d is the diameter of the steel rebar (mm); and l_a is the embedded length of the steel rebar (mm).

The bond strengths obtained from the test results are summarized in Table 3 and the effect of the volume of fly ash on bond strength is shown in Fig. 6. It can be concluded that the peak bond stress values across all the pullout specimens corresponded to slips measured in the range of 0.529-1.273 mm which are significantly higher than the slip values of 0.025 mm and 0.25 mm for the calculation of nominal bond stresses (IS:2770 1967).Compared to normal concrete (i.e., the volume of fly ash is 0), the bond strength

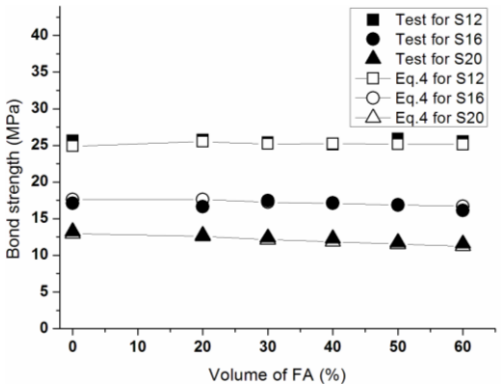

Fig. 7 Comparison of the tested and predicted on bond strength

between fly ash concrete and the steel rebar is closer to each other at the same rebar diameter, irrespective of the fly ash replacement percentage. And the steel rebar diameter has a great impact on bond strength, and test results shows that the bond strength increase conspicuously with the decrease of steel rebar diameter. The steel rebar diameter varies from 12 mm to 25 mm, and the bond strength varies from 25.1 MPa to 11.6 MPa.

3.4 Modeling of the bond strength

At present, many modes have been used to evaluate the ultimate bond strength of the steel bars in normal concrete. The American Concrete Institute (ACI) 318 (2008) and the Canadian Standards Association (CSA) CAN3-A23.3 (2004) codes provides equations to calculate the minimum required bond strength as

$$\tau = \frac{f_y A_b}{\pi d_b l_d} \tag{2}$$

where f_y is the specified yield strength of the tested rebar, and A_b is the area of the tested rebars; d_b is the diameter of the steel rebar; and l_d is the embedded length of the steel rebar.

Australian Standard 3600 (1994) recommended the following equation

$$\tau = 0.265\sqrt{f_c'}\left(\frac{c}{d_b} + 0.5\right) \tag{3}$$

where f'_c is the compressive strength of the cylindrical concrete prism, and c is the radius of a cylindrical; d_b is the diameter of the steel rebar.

However, the modeling of the bond strength for high volume fly ash concrete and steel rebar hasn't been proposed yet. So in this study, the calculation model of the bond strength between concrete and steel rebar adopted by Chinese Code GB50010 (2010), is modified. The calculation bond strength of the steel rebar in high volume fly ash concrete is approximated by the following equation

$$\tau = m(0.82 + \frac{0.9}{l_a / d})(1.6 + 0.7\frac{c}{d} + 20\rho_{sv}) f_t \tag{4}$$

Table 4 Regression parameters a and b

Specimen ID	a	b
S12F0	0.21	0.06
S12F20	0.21	0.08
S12F30	0.21	0.10
S12F40	0.21	0.12
S12F50	0.21	0.14
S12F60	0.21	0.15
S16F0	0.24	0.17
S16F20	0.24	0.18
S16F30	0.24	0.22
S16F40	0.24	0.25
S16F50	0.24	0.24
S16F60	0.24	0.30
S20F0	0.37	0.08
S20F20	0.37	0.08
S20F30	0.37	0.05
S20F40	0.37	0.05
S20F50	0.37	0.07
S20F60	0.37	0.06

In Eq. (4), the parameter m is the influence factor about the effects of the volume of fly ash on bond strength; l_a is the embedded length of the steel rebar; d is the diameter of steel rebar; c is the thickness of concrete cover; ρ_{sv} is the volumetric ratio of the transverse steel rebar; f_t is the concrete splitting tensile strength.

Based on the experimentally obtained bond strength of steel rebar in high volume fly ash concrete, the parameter m was obtained by a data regression analysis. The results are given as follows

$$m = (2.187 - 0.049d) + (1.086 - 0.054d)r \tag{5}$$

where d is the diameter of steel rebar; r is the fly ash replacement percentage.

Fig. 7 shows the comparison of tested and predicted bond stress values. It shows that the developed mode can predict the bond strength of HVFAC reasonably well.

3.5 Model for bond-slip relationship

Modeling of bond-slip relation improve the numerical analysis on reinforced concrete members. As can be seen from Figs. 3-5, the shape of a typical bond-slip curve for HVFAC is similar with the curve of NAC. The curve comprises of an ascending branch and a descending branch, and the normalized bond-slip relationship of HVFAC can be approximately expressed as

$$\bar{\tau} = \begin{cases} \left(\bar{s}\right)^a & \bar{s} \le 1 \\ \dfrac{\bar{s}}{b(\bar{s}-1)^2 + \bar{s}} & \bar{s} > 1 \end{cases} \tag{6}$$

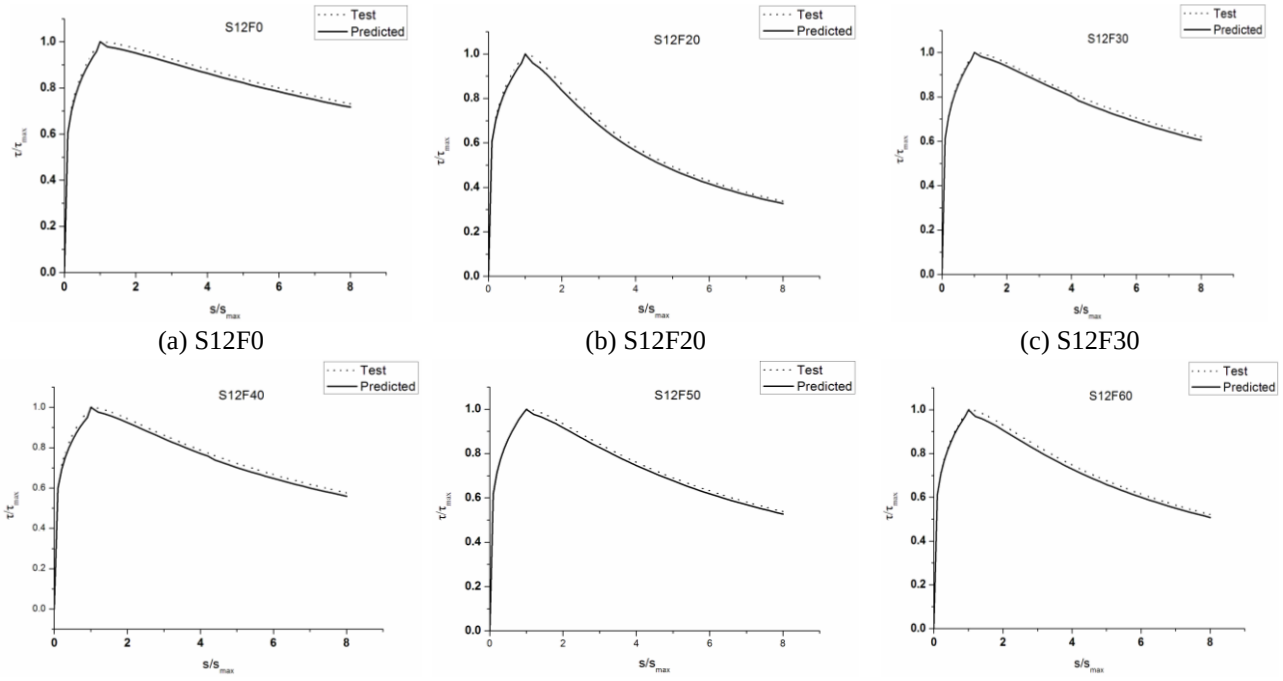

(a) S12F0 (b) S12F20 (c) S12F30

(d) S12F40 (e) S12F50 (f) S12F60

Fig. 8 The tested and predicted bond-slip relationship for the 12 mm dia. steel bars

In Eq. (6), $\bar{\tau} = \tau / \tau_{\max}$, $\bar{s} = s / s_{\max}$, τ_{max} is the peak bond stress and s_{max} is the slip corresponding to the τ_{max}. The parameter *a*, *b* are constants to be determined. In Eq. (6), the first expression suggested by Haraji (1994), and the second expression suggested by Guo (1997). By using a data regression program, the value of the parameter *a*, *b* are computed and are given in Table 4.

The test bond-slip curves and the predicted bond-slip curves provided by Eq. (6) for the 12 mm diameter steel bar in HVFAC are shown in Fig. 8. It can be seen that the predicted curves are fitting well to the test curves, so this equation can be used for predictive assessment of the bond-slip behaviour of HVFAC.

5. Conclusions

Based on the experimental results, the following conclusions can be drawn:

• With the volume of fly ash in concrete increase, the compressive strength and splitting tensile strength of fly ash concrete specimens declines.

• The general shape of the bond-slip curve between fly ash concrete and steel rebar is similar to that for the normal concrete and steel rebar, which includes micro-slip, internal cracking, descending .

• The bond strength between fly ash concrete and the steel rebar is closer to each other at the same rebar diameter, irrespective of the fly ash replacement percentage. And the steel rebar diameter has a great impact on bond strength, and test results show that the bond strength increase conspicuously with the decrease of steel rebar diameter.

• Taking into account the effects of volume of fly ash, a bond strength revised from GB50010 mode is proposed.

Equations for complete bond-slip relationship between fly ash concrete and steel rebar is given, which could be used for predictive assessment of the bond-slip behaviour of high volume fly ash concrete and steel rebar.

Acknowledgments

This work was supported by the Chinese National Natural Science Foundation (No. 51368001), the Natural Science Foundation of Jiangxi Province for Distinguished Young Scholars (No.20162BCB23051), the Technology Support Project of Jiangxi Province (No. 20161BBH80045), and the Open Project Program of Jiangxi Engineering Research Center of Process and Equipment for New Energy, East China Institute of Technology (No.JXNE-2014-08), which are gratefully acknowledged.

References

ACI Committee 318 (2008), *Building Code for Structural Concrete (318R-2008) and Commentary*, American Concrete Institute, Farmington Hills, U.S.A.

AS3600 (1994), *Australian Standard for Concrete Structures*, North Sydney, Australia.

Assi, L.N., Deaver, E., ElBatanouny, M.K. and Ziehl, P. (2016), "Investigation of early compressive strength of fly ash-based geopolymer concrete", *Constr. Build. Mater.*, **113**(15), 369-375.

Chinese Code for the Design of Reinforced Concrete Structures (2010), Chinese Building Construction Publishing Press, Beijing, China.

Chousidis, N., Rakanta, E., Ioannou, I. and Batis, G. (2015), "Mechanical properties and durability performance of reinforced concrete containing fly ash", *Constr. Build. Mater.*,

101(1), 810-817.
CSA CAN3-A23.3 (2004), *Design of Concrete Structures*, Canadian Standards Association, Rexdale, Ontario, Canada.
Deng, Z.C., Jumbe, R.D. and Yuan, C.X. (2014), "Bonding between high strength rebar and reactive powder concrete", *Comput. Concrete*, **13**(3), 411-421.
IS2770 (1967), *Methods of Testing Bond in Reinforced Concrete Part 1, Pull-Out Test*, Bureau of Indian Standards, New Delhi, India.
Junaid, M.T., Khennane, A. and Kayali, O. (2015), "Performance of fly ash based geopolymer concrete made using non-pelletized fly ash aggregates after exposure to high temperatures", *Mater. Struct.*, **48**(10), 3357-3365.
Leung, H.Y., Kim, J., Nadeem, A., Jaganathan, J. and Anwar, M.P. (2016), "Sorptivity of self-compacting concrete containing fly ash and silica fume", *Constr. Build. Mater.*, **113**(15), 369-375.
Nath, P. and Sarker, P.K. (2015), "Use of OPC to improve setting and early strength properties of low calcium fly ash geopolymer concrete cured at room temperature", *Cement Concrete Compos.*, **55**, 205-214.
Shafigh, P., Nomeli, M.A., Alengaram, U.J., Mahmud, H.B. and Jumaat, M.Z. (2016), "Engineering properties of lightweight aggregate concrete containing limestone powder and high volume fly ash", *J. Clean Prod.*, **135**(1), 148-157.
Shen, D.J., Shi, X., Zhu, S., Duan, X.F. and Zhang, J.Y. (2016), "Relationship between tensile Young's modulus and strength of fly ash high strength concrete at early age", *Constr. Build. Mater.*, **123**(1), 317-326.
Tang, C.W. (2015), "Local bond stress-slip behavior of reinforcing bars embedded in lightweight aggregate concrete", *Comput. Concrete*, **16**(3), 449-466.
Wang, X.Y. and Park, K.B. (2015), "Analysis of compressive strength development of concrete containing high volume fly ash", *Constr. Build. Mater.*, **98**(15), 810-819.

CC